

Hypogonadotropic hypogonadism and cleft lip and palate caused by a balanced translocation producing haploinsufficiency for *FGFR1*

HG Kim, S R Herrick, E Lemyre, S Kishikawa, J A Salisz, S Seminara, M E MacDonald, G A P Bruns, C C Morton, B J Quade, J F Gusella

J Med Genet 2005;42:666–672. doi: 10.1136/jmg.2004.026989

We have established the Developmental Genome Anatomy Project (DGAP; //dgap.harvard.edu) to take advantage of the unique opportunity to locate genes of developmental importance provided by apparently balanced chromosomal rearrangements associated with phenotypic abnormalities. By positional cloning at or near the breakpoints, we aim to identify the crucial disease genes whose functions have been disrupted by rearrangement.¹ Kallmann's syndrome (KS) is a developmental disorder characterised by anosmia resulting from agenesis of the olfactory lobes and hypogonadism secondary to deficiency of hypothalamic gonadotropin releasing hormone (GnRH). Its prevalence has been estimated at 1/10 000 in males and 1/50 000 in females. In a minority of cases there are inactivating mutations of *KALI*, an X linked gene encoding a putative adhesion molecule thought to mediate embryonic neuronal migration.^{2–3} Constitutional autosomal chromosome translocations associated with KS have been reported, but the disrupted genes have not been identified.^{4–6}

We have studied a white male subject with a de novo balanced translocation between chromosomes 7, in band p12.3, and 8, in band p11.2 (fig 1A), who was diagnosed on clinical examination to have hypogonadotropic hypogonadism (infantile testes), azoospermia, and cleft lip and palate, without frank anosmia. As a KS patient with a microdeletion involving the same 8p11.2 region had been reported, we sought to identify the chromosome 8 gene disrupted in this reciprocal translocation as a likely candidate for the cause of autosomal KS as well as of isolated hypogonadotropic hypogonadism.⁷ While this breakpoint in *FGFR1* was being characterised, Dodé *et al* identified *FGFR1* mutations in several patients, establishing that disruption of *FGFR1* can cause autosomal dominant KS.⁸

METHODS

This study was approved by the Institutional Review Board of Partners Healthcare Inc, encompassing both the Massachusetts General Hospital and the Brigham and Women's Hospital.

Case report

The subject is a white man who was aged 24 years at the time of initial diagnosis. He had a history of cleft palate, corrected by surgery. He had no outstanding medical problems other than delayed sexual development and a feminine sounding voice. He had his growth spurt at age 18–19 years, developed sparse armpit hair at age 20, and penile hair at 16–17, but no penile or testicular enlargement. He displayed child-like facial hair, sparse axillary adult appearing hair, and prepubertal chest hair. Based on the presence of cleft palate and hypogonadism, a tentative diagnosis of Kallmann's syndrome was reached, though the subject did not complain

Key points

- Kallmann's syndrome (KS), characterised by hypogonadotropic hypogonadism and anosmia, can be caused by inactivating mutations of the X linked *KALI* gene, but these mutations account for less than 15% of KS patients. The remaining cases, as well as cases of hypogonadotropic hypogonadism without anosmia, are believed to be caused by mutations at two or more autosomal loci, including a segment of 8p heterozygous for a microdeletion in one KS patient.
- Recently, mutation in *FGFR1*, the 8p gene encoding fibroblast growth factor receptor 1, has been shown to cause autosomal dominant KS. We report positional cloning of the genomic breakpoints of the balanced reciprocal translocation t(7;8)(p12.3;p11.2) from a male patient with hypogonadotropic hypogonadism and cleft lip and palate. The translocation disrupts *FGFR1* (MIM 136350) between exons 2 and 3 and predicts a novel fusion gene product.
- Although various *FGFR1* translocations producing fusion proteins have been reported as causes of myeloproliferative disorders, this is the first case in which a constitutional *FGFR1* translocation is associated with a developmental disorder.

of anosmia. He was prescribed a regimen of testosterone injections, which successfully induced secondary sexual characteristics. At the age of 31, he was seen by a different physician for azoospermia and infertility, and cytogenetic analysis was ordered for the possibility of Klinefelter's syndrome. The analysis revealed an apparently balanced chromosomal translocation with the karyotype, 46,XY,t(7;8)(p12.3;p11.2). Informed consent for the generation of a lymphoblastoid cell line was obtained in accordance with institutional policies.⁹

Fluorescent in situ hybridisation analysis

Breakpoint mapping on chromosome 8 was initiated using clones placed on the cytogenetic map by fluorescent in situ hybridisation (FISH) analysis and on the sequence map by sequence tagged sites.¹⁰ Metaphase chromosomes from the patient cell line were prepared for analysis by GTG banding or FISH using standard protocols. Briefly, clones for FISH were

Abbreviations: FGF, fibroblast growth factor; FISH, fluorescent in situ hybridisation; KS, Kallmann's syndrome; SSCP, single strand conformation polymorphism; UCSC, University of California Santa Cruz

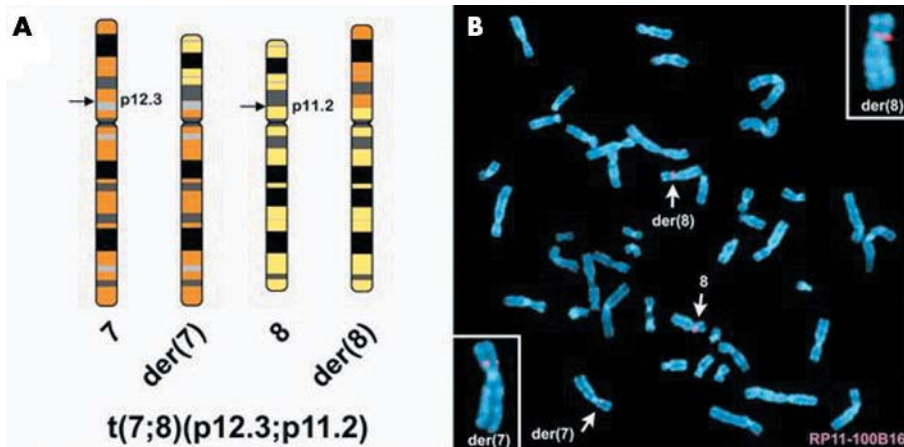


Figure 1 Fluorescent in situ hybridisation (FISH) mapping of the chromosome 8 breakpoint. (A) Ideogram illustrating the balanced $t(7;8)(p12.3;p11.2)$ in the patient. (B) FISH mapping with RP11-100B16, labelled with SpectrumOrange, resulted in hybridisation to the normal chromosome 8, and the der(8) and der(7) derivative chromosomes. The insets present the derivative chromosomes at higher magnification.

selected using genome maps provided by the National Center for Biotechnology Information and the University of California Santa Cruz (UCSC) Genomics Bioinformatics Group.^{10–11} Bacterial artificial chromosome (BAC) clones were obtained from CITB-D and RP11 libraries (Invitrogen, San Diego, California, and the Children's Hospital of Oakland Research Institute) and directly labelled with SpectrumOrange or Green-dUTP (Vysis) by nick translation. Hybridisations were carried out according to manufacturers' protocols. Metaphase chromosomes were counterstained with 4,6-diamino-2-phenylindole-dihydrochloride (DAPI), and at least 10 metaphases were analysed using a Zeiss Axioskop microscope. Images were captured with the CytoVision system (Applied Imaging, San José, California, USA). The karyotype, 46,XY,t(7;8)(p12.3;p11.2), was reconfirmed by GTG banding before breakpoint mapping by FISH.

Mapping and cloning of breakpoints

Southern blot analysis of patient lymphoblast genomic DNA with probes D011-A, D011-B, and D011-C to search for altered restriction fragments was carried out using standard protocols. For each lane, 10 μ g of genomic DNA from the patient and control were digested with an appropriate restriction enzyme. Fragments were separated on a 1.0% agarose gel and transferred to Hybond-N membrane (Amersham, Arlington Heights, Illinois, USA). Filters were ultraviolet cross linked, baked at 80°C, and hybridised with probes labelled with ³²P-dCTP by random priming. Hybridisation of labelled fragments was done in the presence of excess herring sperm competitor DNA, and hybridised membranes were washed at 60°C with 0.15 M NaCl/0.015 M sodium citrate/0.1% sodium dodecyl sulphate (SDS) for 30 minutes. Autoradiography took place for 16 hours at –70°C using two intensifying screens. Three hybridisation probes were amplified by the following primer sets:

D011-A: 5'CTGTCAGGGTTCCATCACC3'+5'CCTAGAAACC TCCGTGTG3'; D011-B: 5'GTGGCTCTGTTCTATCCCTC3'+5'CAACAGTCATGGGAACCATC3'; D011-C: 5'GCACCTAGAG CCTGTAATAG3'+5'TGTCCAAGTCTCTCCTCGGA3'.

A 1.6 kb *Bam*HI junction fragment from der(8) was amplified by suppression polymerase chain reaction (PCR) using the following primer sets: 5'CCTAATACGACTCAC TATAGG3'+5'GCAATGCACTGTAAACACATG3'; 5'CTATAGG GCTCGAGCGGC3'+5'CCTAGAGCCTGTAATAGTAA3'.¹² Then, the der(7) junction fragment was amplified by nested PCR using the primer sets: 5'GGATCATTAGAGGGATTCCGAA3'+

5'GCAAGCTGTGCTGGAAGCA3'; 5'CCAGCTTCACAGGTG TTTC3'+5'CCAGCATTGAAGAGGGAGT3'.

Fusion transcript amplification

Total RNA was isolated from patient and control lymphoblastoid cell lines with the RNeasy Mini Kit (Qiagen, Valencia, California, USA). Reverse transcription of total RNA (1 μ g) was undertaken by using either random hexanucleotide priming and Superscript II (Gibco BRL, Gaithersburg, Maryland, USA) or the SMART-PCR cDNA synthesis kit (Clontech, Palo Alto, California, USA) according to the protocols provided. In each experiment, DNA contamination was excluded by the absence of a PCR product in the sample without reverse transcriptase, amplified under the same conditions as the reverse transcribed RNA sample. Nested PCR was carried out using *Pfu* polymerase (Gibco BRL) with the following primer sets, annealing at 56°C for 30 seconds with an extension for one minute 40 seconds: *TENS1-FGFR1*: 5'CTGAGAAAGCCCTCAGTGTC3'+5'CAAG ATCTGGACATAAGGCAGG3', 5'GGCAGAGCAGCTACTCC ACA3'+5'GTCACGTGACACCTTACACATGAACTC3'; *FGFR1-TENS1*: 5'CCTCTTGCAGCCACAGGC3'+5'CCTTCAACATGGC GATGG3', 5'GCAGCGCGGAG3'+5'CCTGTACCAGAACTT GGAAGTG3'.

Mutation analysis

Mutation analysis of the second allele of *FGFR1* was done by single strand conformation polymorphism (SSCP). In all, 24 genomic fragments including the entire coding region, UTR, and intron–exon boundaries were amplified from 18 exons of *FGFR1* by PCR with [³²P]-dCTP. Primers were designed to amplify genomic fragments with the size of 200 to 300 base pairs (bp) (primer sequences and amplification conditions are available on request). PCR products were applied on non-denaturing 8% glycerol gels with electrophoresis overnight at room temperature and 8W constant power. PCR products that displayed a banding pattern different from control samples were sequenced by an ABI Prism 377/XL DNA sequencer (Applied Biosystems, Foster City, California, USA).

RESULTS

Delineation of the breakpoint region on 8p11.2

To identify the genes potentially disrupted in the patient, we first mapped the translocation breakpoints using FISH. Two BAC clones selected from the UCSC map as starting clones for FISH—GS1-211B7 and GS1-165D4 from 8p12 and 8p11.2—mapped telomeric and centromeric to the breakpoint,

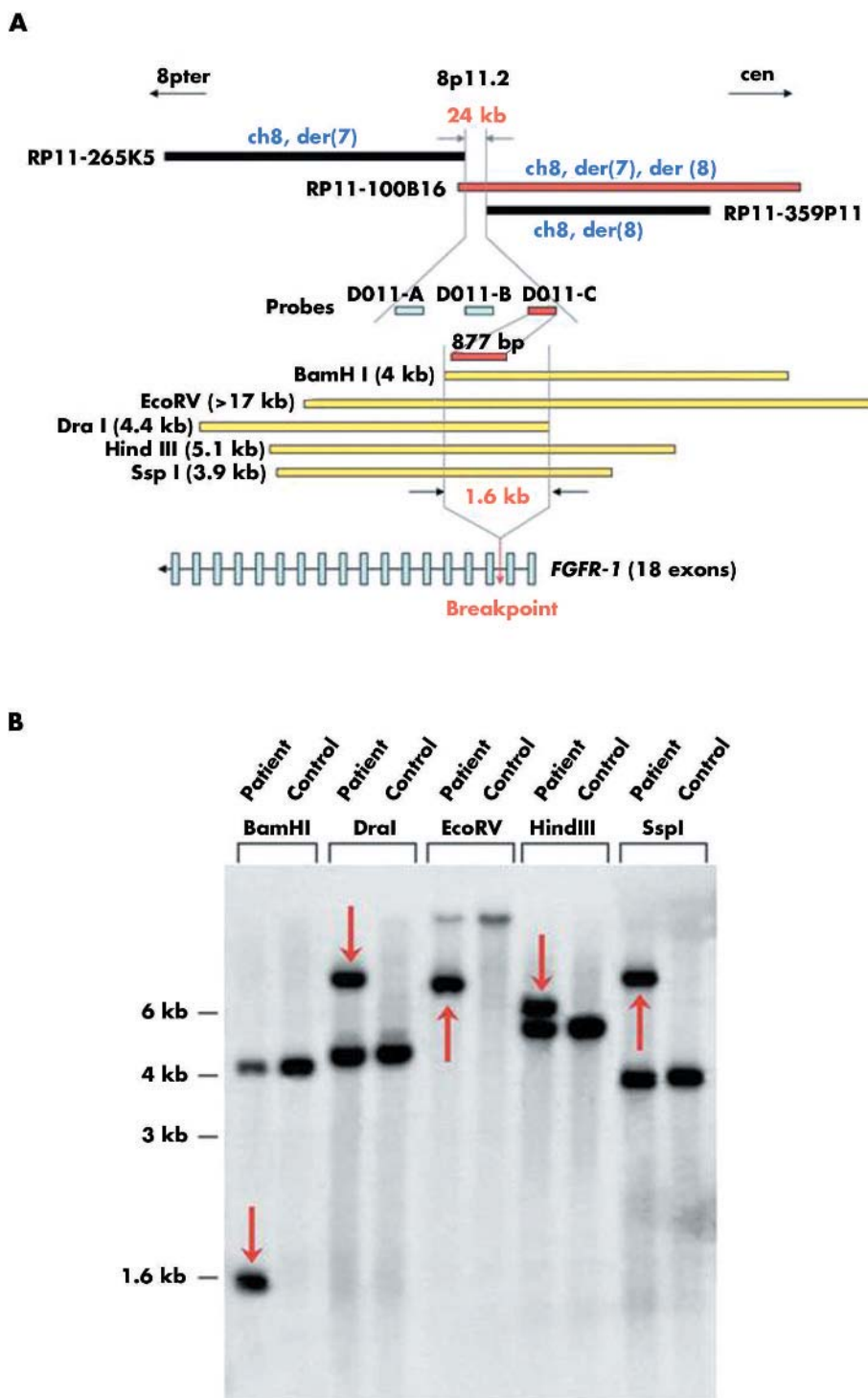


Figure 2 (A) Schematic presentation of positional cloning on chromosome 8. The 24 kb breakpoint region determined by fluorescent in situ hybridisation (FISH) was further narrowed to 1.6 kb by Southern blot hybridisation, which detected junction fragments with five different restriction enzymes. The breakpoint is located between exons 2 and 3 of *FGFR1*. The *FGFR1* gene is not to scale. (B) Southern blot hybridisation of genomic DNA from the translocation patient with 877 bp probe D011-C from intron 2 of *FGFR1*. Note the detection of five altered fragments caused by the translocation junction, generated by enzymes BamHI, DraI, EcoRV, HindIII, and SspI. C, genomic DNA from karyotypically normal control; P, patient genomic DNA.

respectively, showing that the chromosome 8 breakpoint was contained in a 12 Mb region. Subsequent experiments were carried out using BACs chosen from within this region to narrow the candidate region until a breakpoint crossing BAC clone was identified. Seventeen BACs were examined, of

which eight were proximal to the breakpoint and nine distal. The final BAC, RP11-100B16, hybridised to the normal chromosome 8, and both der(7) and der(8) chromosomes, indicating that it spans the translocation breakpoint (fig 1B). Additionally two BAC clones that partially

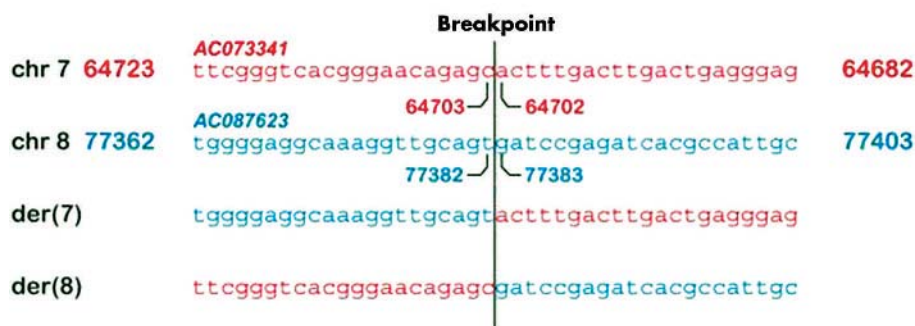


Figure 3 Genomic DNA sequence at two breakpoints from two junction fragments. The breakpoint on chromosome 7 is located between nucleotides 64702 and 64703 of AC073341, while on chromosome 8 it occurs between nucleotides 77382 and 77383 of AC087623. Note no gain or loss of nucleotides at the two breakpoints of the derivative chromosomes, showing a perfectly balanced reciprocal translocation.

overlap with RP11-100B16—RP11-265K5 and RP11-359P11—mapped distal and proximal to the breakpoint, respectively (fig 2A). Based on the sequence of these BACs, the location of the breakpoint region was confined to ~24 kb of DNA.

Southern blot hybridisation and cloning of the breakpoints on 8p11.2

To localise the breakpoint region in 8p11.2 further, three DNA fragments—D011-A, D011-B, and D011-C—were amplified by PCR from the narrowed 24 kb region (fig 2A) and used to probe patient DNA on genomic blots. D011-B and D011-C both detected altered restriction fragments due to the translocation (fig 2B), narrowing the breakpoint to 1557 bp on the BAC restriction map and suggesting that the breakpoint is between exons 2 and 3 of *FGFR1* isoform 1 (fig 2A). We cloned and sequenced junction fragments spanning the breakpoints from both derivative chromosomes, which revealed that the translocation is perfectly balanced, without the gain or loss of any sequence. The sequences of the breakpoint regions for the der(7) and der(8) chromosomes are given in fig 3.

Delineation of the breakpoint region on 7p12.3

BAC clones RP11-183O1 from 7p22.1 and RP11-34J24 from 7p11.2 were used as starting clones for FISH, and mapped distal and proximal to the breakpoint, respectively, indicating that the chromosome 7 breakpoint was contained in a 49 Mb region. Using randomly selected BACs, the breakpoint region was narrowed to ~1.3 Mb, flanked by RP11-126K7 and RP11-271O10, which map telomeric and centromeric to the breakpoint, respectively. After the breakpoint was cloned and sequenced, on the basis of the chromosome 8 findings (see below) the junction sequence was found to be located in RP11-549I23. This was confirmed by FISH, showing three signals, one each on chromosome 7 and both derivative chromosomes (data not shown).

TENS1 in 7p12 and *FGFR1* in 8p11 are disrupted

The chromosome 7 breakpoint lies in intron 15 of *TENS1* (AF417489, 1445 amino acids, between nucleotides 64702 and 64703 of GenBank entry AC073341, 15665 bp downstream of exon 15), while the breakpoint on chromosome 8 is in intron 2 of *FGFR1* (NM_000604, 822 amino acids, between nucleotides 77382 and 77383 of GenBank entry AC087623, 22414 bp downstream of exon 2). The chromosome 8 breakpoint maps within a SINE/Alu repetitive sequence while the breakpoint in *TENS1* occurs in unique intronic sequence with no apparent homology to the chromosome 8 breakpoint region.

Fusion transcript amplification

The location of the translocation breakpoint predicts two putative reciprocal in-frame fusion transcripts *TENS1/FGFR1* and *FGFR1/TENS1* (fig 4A). On the derivative chromosome 7, exons 1–15 of *TENS1* are predicted to join with exons 3–18 of *FGFR1* isoform 1 and to form a 5891 bp *TENS1Δex16-26/FGFR1Δex1-2* transcript that spans 31 exons and encodes 1675 amino acids without frameshift, from the normal *TENS1* initiation codon (ATG) in exon 1 to the termination codon (TGA) in exon 31 (corresponding to the normal stop codon in *FGFR1* exon 18). The putative fusion protein would consist of the first 883 amino acids of *TENS1* joined to the final 792 amino acids of *FGFR1* (fig 4, panels A and B).

On the derivative chromosome 8, exons 1–2 of *FGFR1* are joined to exons 16–26 of *TENS1*, predicting a 2546 bp *FGFR1Δex3-18/TENS1Δex1-15* transcript that comprises 13 exons and encodes 592 amino acids. Again there is no frameshift, as the start codon and stop codon occur at exon 2 and exon 13, respectively, at the same positions as the corresponding exon 2 of *FGFR1* and exon 26 of *TENS1*. The predicted *FGFR1-TENS1* fusion protein would contain the first 30 amino acids of *FGFR1* followed by the final 562 amino acids of *TENS1* (fig 4, panels A and B).

To establish whether either fusion transcript is expressed in a lymphoblastoid cell line from the patient, we carried out reverse transcriptase PCR (RT-PCR). Only the *TENS1-FGFR1* fusion transcript was detected (fig 5), but sequencing revealed the skipping of *FGFR1* exon 3, an alternative splicing pattern also seen in several native *FGFR1* encoded isoforms. The 5624 bp *TENS1Δex16-26/FGFR1Δex1-3* transcript encodes a fusion protein of 1586 amino acids comprising the first 883 amino acids of *TENS1* joined to the final 703 amino acids of *FGFR1* (fig 4, panels A and B).

Mutation analysis of the non-translocated *FGFR1* allele

Mutation analysis of the second non-translocated *FGFR1* allele from the patient, done by SSCP and direct sequencing, identified only a heterozygous nucleotide difference, 345 C→T in exon 3, a known SNP (NCBI reference SNP ID: rs2915665) which does not alter the Ser amino acid encoded at this site. Thus the presence of the translocated allele of the *FGFR1* results in a disease phenotype without a corresponding coding sequence mutation in the alternate *FGFR1* allele.

DISCUSSION

The *TENS1* locus encodes tensin-like SH2 domain-containing protein 1 (also known as tumour endothelial marker 6, tensin 3), a 1445 amino acid protein named for its similarity with tensin, an actin filament crosslinking protein found in focal adhesions.^{13 14} *TENS1* protein contains a protein tyrosine

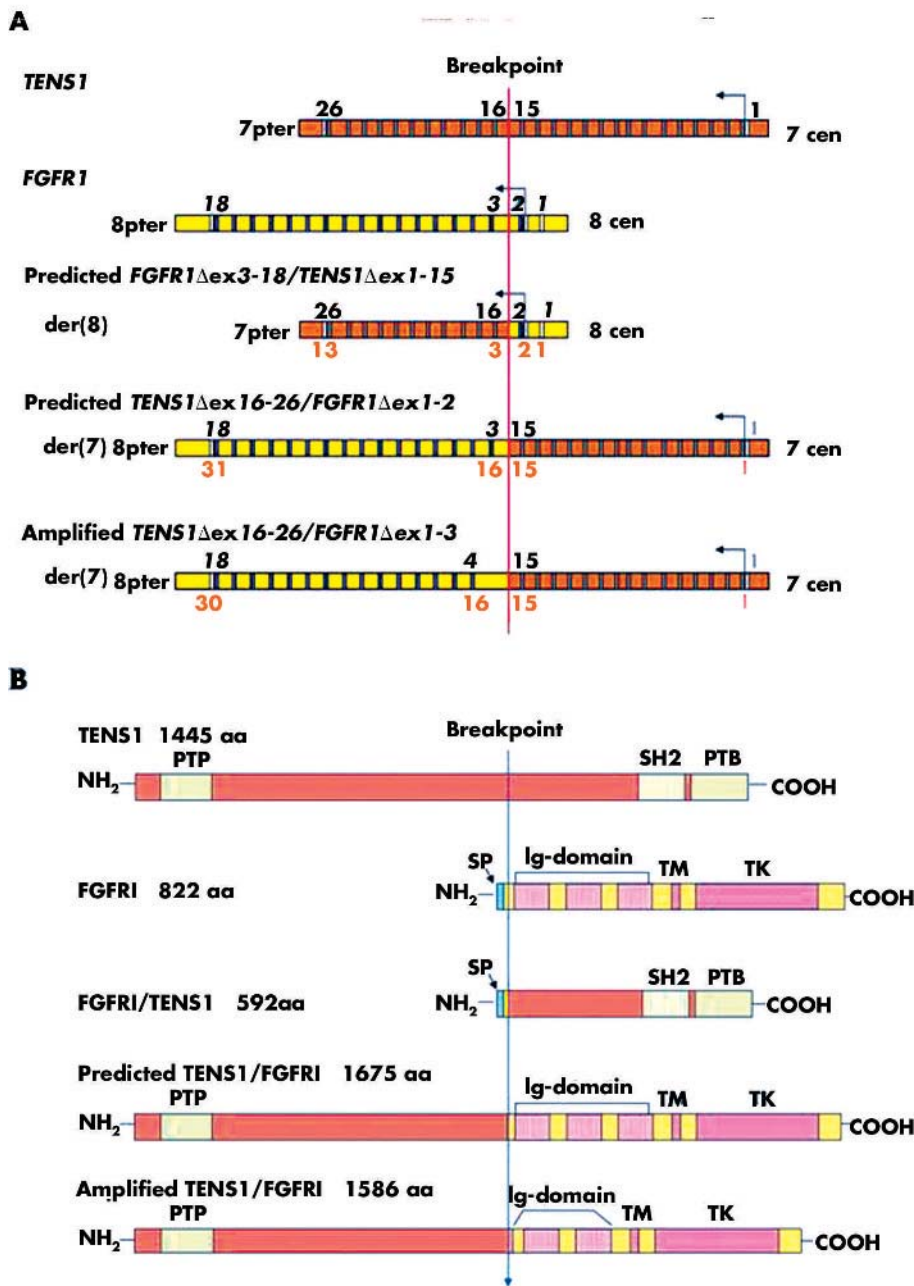


Figure 4 (A) Disruption of genes *FGFR1* and *TENS1* by t(7;8), resulting in two in-frame fusion genes. White boxes indicate 5' and 3' untranslated regions of exons. *TENS1* and *FGFR1* coding exons are shown as grey boxes and blue boxes, respectively, numbered above the gene in the same colour, whereas exons of fusion genes are numbered in orange below the gene. Note that the stop codons of the two fusion genes are at the same exon locations as in the corresponding wild-type genes, as there is no frameshift. In the amplified *TENS1*-*FGFR1* fusion transcript, exon 3 of *FGFR1* is skipped. Notable exons are numbered and the direction of gene transcription is indicated by arrows. The sizes of exons and introns is not to scale. (B) *TENS1*, *FGFR1*, *FGFR1*-*TENS1*, and *TENS1*-*FGFR1* protein domains. In the amplified fusion protein *TENS1*-*FGFR1*, the transmembrane domain (TM), and tyrosine kinase domain (TK) of *FGFR1* are not affected by the translocation, but the signal peptide (SP) of *FGFR1* and the first immunoglobulin (Ig) like domain are absent. The translocation does not directly disrupt the amino terminal protein tyrosine phosphatase domain (PTP) or the carboxyl terminal Src homology 2 (SH2) and phosphotyrosine binding (PTB) domains of *TENS1*, but does segregate the coding sequences for these domains to different fusion transcripts.

phosphatase domain in the amino-terminal region and Src homology 2 (SH2) and phosphotyrosine binding domains near its carboxyl-terminus. *FGFR1* encodes several different isoforms of a transmembrane protein, the extracellular moiety of which interacts with fibroblast growth factors (FGFs), setting in motion a cascade of downstream signals, ultimately influencing mitogenesis and differentiation; it is characterised by two or three extracellular immunoglobulin-like loops (depending on inclusion of exon 3), a transmembrane domain, and an intracellular tyrosine kinase domain.

The predicted *TENS1*/*FGFR1* fusion protein lacks the *FGFR1* signal peptide and the first Ig-like domain, but contains Ig-like domains 2 and 3, which are sufficient for specific FGF binding, and an intact tyrosine kinase domain region, suggesting the potential for functionality (fig 3B).¹⁵

However, the related KS phenotype in a patient hemizygous for 8p due to the deletion region suggests that the translocation produces hypogonadotropic hypogonadism as a result of haploinsufficiency for *FGFR1*.⁷ Consistent with this view, there was no evidence for an *FGFR1* mutation on the second allele in SSCP/sequence analysis in any of 18 exons and splice junctions. The apparent functional hemizygosity for *FGFR1* in the translocation patient probably reflects a failure to direct the *FGFR1* functional domains to the proper location in the plasma membrane owing to the absence of the appropriate signal peptide and the presence of the large *TENS1* moiety. While this work was being completed, Dodé *et al*, and subsequently Sato *et al*, reported several truncating and missense *FGFR1* mutations in KS patients, some with cleft lip and palate, consistent with the haploinsufficiency in

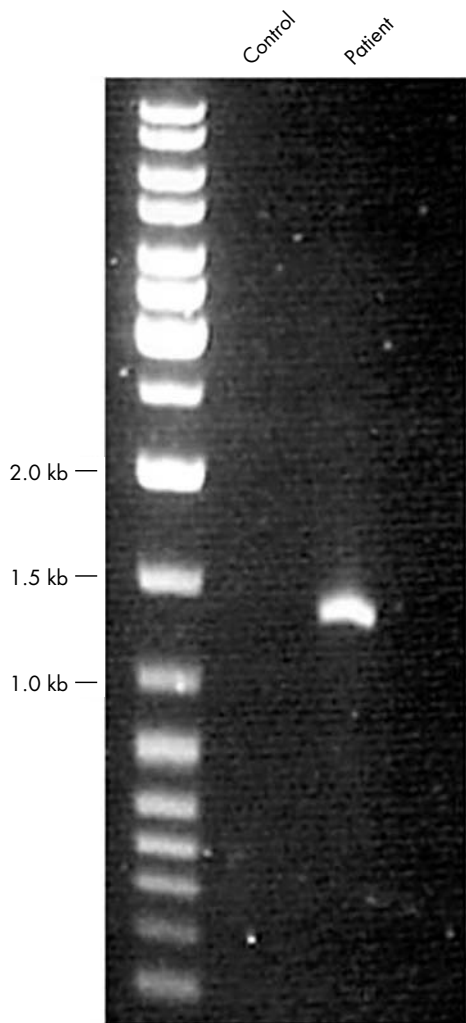


Figure 5 Expression of the fusion gene *TENS1*^{ex16-26}/*FGFR1*^{ex1-3}. Nested RT-PCR was performed by using forward primers in exon 15 of *TENS1* and reverse primers in exon 7 of *FGFR1*. Reverse transcribed $\hat{t}(7;8)$ patient RNA, but not RNA from a normal individual (control), resulted in amplification of a fusion transcript of 1.4 kb smaller than the expected size of 1.7 kb. The sequence analysis of this amplified fusion gene from the patient confirmed the skipping of exon 3 of *FGFR1*.

the patient reported here.^{8 16} However, the absence of frank anosmia in the current patient indicates that sufficient *FGFR1* function may have been maintained to prevent the degree of agenesis of the olfactory lobes typical in KS.

As the translocation patient displays no obvious phenotypes distinct from those seen in patients with KS associated *FGFR1* point mutations, the disruption of *TENS1* does not seem to contribute to the patient's abnormalities. This suggests that heterozygous inactivation of *TENS1* is without dramatic consequence, but the possibility that the predicted fusion proteins effectively provide normal *TENS1* function cannot be excluded.

The X linked form of KS is associated with inactivating mutation of the *KALI* gene, encoding anosmin 1, a secreted proteoglycan binding protein with similarities to neuronal cell adhesion molecules.^{3 17} Anosmin 1 interacts with heparan and chondroitin sulphates to promote cell adhesion and neuronal outgrowth, and has been implicated in the migration of gonadotropin releasing hormone (GnRH) producing neurones and olfactory axonal fibres, though the receptor system through which it acts remains uncertain.¹⁸ Notably, *FGFR1* activation by binding to FGF ligands involves

receptor dimerisation that also requires heparan sulphate proteoglycan binding.¹⁹ Indeed, FGF2 ligand and *FGFR1* have been co-crystallised with heparin, and the structure of the complex defined.²⁰ The common association with heparan sulphates and the similar effects of *KALI* and *FGFR1* inactivating mutations support the suggestion that the *FGFR1* signalling pathway participates directly in mediating anosmin 1 function.^{8 21}

The translocation patient reported here and the KS patients reported by others also support the view that haploinsufficiency for *FGFR1* is a cause of cleft lip and palate.^{7 8 16} Interestingly, *FGFR1* gain of function mutations have previously been associated with the craniosynostosis of Pfeiffer's syndrome and in the Jackson-Weiss syndrome.^{22 23} These syndromes can also be caused by mutations in *FGFR2*, which has also been associated with cleft palate in Apert's syndrome, indicating that the two receptors may function in the same signalling pathway.²⁴ This suggests that *FGFR2*, located at 10q26, may be an excellent candidate for an additional KS or idiopathic hypogonadotropic hypogonadism locus. Hence it would be of interest to determine whether *FGFR2* is disrupted by translocation in a KS patient with a de novo unbalanced *der(1)t(1;10)(q44;q26)*.⁴

It is noteworthy that a variety of fusion proteins involving *FGFR1* underlie the 8p11 myeloproliferative syndrome (EMS)/stem cell leukaemia-lymphoma syndrome, presumably because of constitutive activity of the tyrosine kinase domain.²⁵⁻²⁹ However, neither Pfeiffer's syndrome nor the Jackson-Weiss syndrome shows a myeloproliferation defect, suggesting that the gain of function in these cases is insufficient or inappropriate to transform target cells. The constitutional translocation reported here creates a predicted fusion protein that has not produced a myeloid disorder, despite being likely to mislocalise a portion of *FGFR1* containing the tyrosine kinase domain. This reinforces the view that both the fusion partner and the site of the breakpoint are likely to be critical in producing constitutive tyrosine kinase activity in a manner that leads to malignancy. This is the first demonstration that constitutional translocation of *FGFR1* can lead to abnormal development rather than to myeloid disorder, and provides a basis for more detailed structure-function comparison of the respective fusion proteins.

ELECTRONIC DATABASE INFORMATION

GenBank accession numbers: *FGFR1*, AC087623, NM_000604; *TENS1*, AC073341, AF417489.
dbSNP information: rs2915665.

ACKNOWLEDGEMENTS

We are indebted to Carolyne Rooryck and Robert E Eisenman for technical assistance, Amy Bosco and Heather L Ferguson for obtaining informed consent and clinical information, Wenqi Zeng and Jo-Chen Chou for technical advice, Tammy Gillis, Michelle Flores, and the MGH Genomics Core Facility for DNA sequence analysis and Francesca Puglisi for cell culture and genomic DNA extraction. This work was supported by USPHS grants GM061354 (Developmental Genome Anatomy Project) and HD28138.

Authors' affiliations

HG Kim, S Kishikawa, M E MacDonald, J F Gusella, Molecular Neurogenetics Unit, Center for Human Genetic Research, Massachusetts General Hospital/Department of Genetics, Harvard Medical School, Boston, Massachusetts, USA

S R Herrick, B J Quade, Department of Pathology, Brigham and Women's Hospital/Harvard Medical School

E Lemyre, Medical Genetics Service, Hôpital Ste Justine, University of Montreal, Montreal, Canada

J A Salisz, West Shore Urology, Mercy Drive, Muskegon, Michigan, USA

S Seminara, Reproductive Endocrine Unit, Massachusetts General Hospital

G A P Bruns, Genetics Division, Children's Hospital/Department of Pediatrics, Harvard Medical School

C C Morton, Departments of Obstetrics, Gynecology and Reproductive Biology and Pathology, Brigham and Women's Hospital/Harvard Medical School

Conflicts of interest: none declared.

Correspondence to: Dr James F Gusella, Molecular Neurogenetics Unit, Center for Human Genetic Research, Massachusetts General Hospital/Department of Genetics, Harvard Medical School, CNY149-6214, 13th Street, Boston, Massachusetts 02129, USA; gusella@helix.mgh.harvard.edu

REFERENCES

- Collins FS. Positional cloning moves from perditional to traditional. *Nat Genet* 1995;**9**:347–50.
- Oliveira LM, Seminara SB, Beranova M, Hayes FJ, Valkenburgh SB, Schipani E, Costa EM, Latronico AC, Crowley WF, Vallejo M. The importance of autosomal genes in Kallmann syndrome: genotype-phenotype correlations and neuroendocrine characteristics. *J Clin Endocrinol Metab* 2001;**86**:1532–8.
- Franco B, Guioli S, Pragliola A, Incerti B, Bardoni B, Tonlorenzi R, Carrozzo R, Maestrini E, Pieretti M, Taillon-Miller P, Brown C, Willard H, Lawrence C, Persico M, Camerino G, Ballabio A. A gene deleted in Kallmann's syndrome shares homology with neural cell adhesion and axonal path-finding molecules. *Nature* 1991;**353**:529–36.
- Schinzel A, Lorda-Sanchez I, Binkert F, Carter NP, Bebb CE, Ferguson-Smith MA, Eiholzer U, Zachmann M, Robinson WP. Kallmann syndrome in a boy with a t(1;10) translocation detected by reverse chromosome painting. *J Med Genet* 1995;**32**:957–61.
- Kikuchi I, Nagamine M, Ueda A, Mihara K, Seita M, Minoda M. Chromosomal translocation t(13;16) in a patient with idiopathic hypogonadotropic hypogonadism. *Intern Med* 1993;**32**:465–7.
- Best LG, Wasdahl WA, Larson LM, Sturlaugson J. Chromosome abnormality in Kallmann syndrome. *Am J Med Genet* 1990;**35**:306–9.
- Vermeulen S, Messiaen L, Scheir P, De Bie S, Speleman F, De Paepe A. Kallmann syndrome in a patient with congenital spherocytosis and an interstitial 8p11.2 deletion. *Am J Med Genet* 2002;**108**:315–18.
- Dode C, Levilliers J, Dupont JM, De Paepe A, Le Du N, Soussi-Yanicostas N, Coimbra RS, Delmagnani S, Compain-Nouaille S, Baverel F, Pecheux C, Le Tessier D, Cruaud C, Delpuch M, Speleman F, Vermeulen S, Amalfitano A, Bachelot Y, Bouchard P, Cabrol S, Carel JC, Delemarre-van de Waal H, Goulet-Salmon B, Kottler ML, Richard O, Sanchez-Franco F, Saura R, Young J, Petit C, Hardelin JP. Loss-of-function mutations in FGFR1 cause autosomal dominant Kallmann syndrome. *Nat Genet* 2003;**33**:463–5.
- Anderson MA, Gusella JF. Use of cyclosporin A in establishing Epstein-Barr virus-transformed human lymphoblastoid cell lines. *In Vitro* 1984;**20**:856–8.
- Cheung VG, Nowak N, Jang W, Kirsch IR, Zhao S, Chen XN, Furey TS, Kim UJ, Kuo WL, Olivier M, Conroy J, Kasprzyk A, Massa H, Yonescu R, Sait S, Thoreen C, Snijders A, Lemyre E, Bailey JA, Bruzel A, Burrill WD, Clegg SM, Collins S, Dhani P, Friedman C, Han CS, Herrick S, Lee J, Ligon AH, Lowry S, Morley M, Narasimhan S, Osogawa K, Peng Z, Plajzer-Frick I, Quade BJ, Scott D, Sirotkin K, Thorpe AA, Gray JW, Hudson J, Pinkel D, Ried T, Rowen L, Shen-Ong GL, Strausberg RL, Birney E, Callen DF, Cheng JF, Cox DR, Doggett NA, Carter NP, Eichler EE, Haussler D, Korenberg JR, Marton CC, Albertson D, Schuler G, de Jong PJ, Trask BJ. Integration of cytogenetic landmarks into the draft sequence of the human genome. *Nature* 2001;**409**:953–8.
- Karolchik D, Baertsch R, Diekhans M, Furey TS, Hinrichs A, Lu YT, Roskin KM, Schwartz M, Sugnet CW, Thomas DJ, Weber RJ, Haussler D, Kent WJ. The UCSC Genome Browser Database. *Nucleic Acids Res* 2003;**31**:51–4.
- Siebert PD, Chenchik A, Kellogg DE, Lukanov KA, Lukanov SA. An improved PCR method for walking in uncloned genomic DNA. *Nucleic Acids Res* 1995;**23**:1087–8.
- Carson-Walter EB, Watkins DN, Nanda A, Vogelstein B, Kinzler KW, St Croix B. Cell surface tumor endothelial markers are conserved in mice and humans. *Cancer Res* 2001;**61**:6649–55.
- Chen H, Ishii A, Wong WK, Chen LB, Lo SH. Molecular characterization of human tensin. *Biochem J* 2000;**351**:403–11.
- Plotnikov AN, Schlessinger J, Hubbard SR, Mohammadi M. Structural basis for FGF receptor dimerization and activation. *Cell* 1999;**98**:641–50.
- Sato N, Katsumata N, Kagami M, Hasegawa T, Hori N, Kawakita S, Minowada S, Shimotsuka A, Shishiba Y, Yokozawa M, Yasuda T, Nagasaki K, Hasegawa D, Hasegawa Y, Tachibana K, Naiki Y, Horikawa R, Tanaka T, Ogata T. Clinical assessment and mutation analysis of Kallmann syndrome 1 (KAL1) and fibroblast growth factor receptor 1 (FGFR1, or KAL2) in five families and 18 sporadic patients. *J Clin Endocrinol Metab* 2004;**89**:1079–88.
- Hardelin JP. Kallmann syndrome: towards molecular pathogenesis. *Mol Cell Endocrinol* 2001;**179**:75–81.
- Cariboni A, Pimpinelli F, Colamarino S, Zaninetti R, Piccollella M, Rumio C, Piva F, Rugarli E, Maggi R. The product of X-linked Kallmann's syndrome gene (KAL1) affects the migratory activity of gonadotropin-releasing hormone (GnRH)-producing neurons. *Hum Mol Genet* 2004;**13**:2781–91.
- Ornitz DM. FGFs, heparan sulfate and FGFRs: complex interactions essential for development. *Bioessays* 2000;**22**:108–12.
- Schlessinger J, Plotnikov AN, Ibrahim OA, Eliseenkova AV, Yeh BK, Yayon A, Linhardt RJ, Mohammadi M. Crystal structure of a ternary FGF-FGFR-heparin complex reveals a dual role for heparin in FGFR binding and dimerization. *Mol Cell* 2000;**6**:743–50.
- Dode C, Hardelin JP. Kallmann syndrome: fibroblast growth factor signaling inefficiency? *J Mol Med* 2004;**82**:725–34.
- Muenke M, Schell U, Hehr A, Robin NH, Losken HW, Schinzel A, Pulley LJ, Rutland P, Reardon W, Malcolm S, et al. A common mutation in the fibroblast growth factor receptor 1 gene in Pfeiffer syndrome. *Nat Genet* 1994;**8**:269–74.
- Roscioli T, Flanagan S, Kumar P, Masel J, Gattas M, Hyland VJ, Glass IA. Clinical findings in a patient with FGFR1 P252R mutation and comparison with the literature. *Am J Med Genet* 2000;**93**:22–8.
- Wilkie AO, Morriss-Kay GM. Genetics of craniofacial development and malformation. *Nat Rev Genet* 2001;**2**:458–68.
- Xiao S, Nalabolu SR, Aster JC, Ma J, Abruzzo L, Jaffe ES, Stone R, Weissman SM, Hudson TJ, Fletcher JA. FGFR1 is fused with a novel zinc-finger gene, ZNF198, in the t(8;13) leukaemia/lymphoma syndrome. *Nat Genet* 1998;**18**:84–7.
- Popovici C, Adelaide J, Ollendorff V, Chaffanet M, Guasch G, Jacrot M, Leroux D, Birnbaum D, Pebusque MJ. Fibroblast growth factor receptor 1 is fused to FIM in stem-cell myeloproliferative disorder with t(8;13). *Proc Natl Acad Sci USA* 1998;**95**:5712–17.
- Popovici C, Zhang B, Gregoire MJ, Jonveaux P, Lafage-Pochitaloff M, Birnbaum D, Pebusque MJ. The t(6;8)[q27;p11] translocation in a stem cell myeloproliferative disorder fuses a novel gene, FOP, to fibroblast growth factor receptor 1. *Blood* 1999;**93**:1381–9.
- Guasch G, Mack GJ, Popovici C, Dastugue N, Birnbaum D, Rattner JB, Pebusque MJ. FGFR1 is fused to the centrosome-associated protein CEP110 in the 8p12 stem cell myeloproliferative disorder with t(8;9)[p12;q33]. *Blood* 2000;**95**:1788–96.
- Demiroglu A, Steer EJ, Heath C, Taylor K, Bentley M, Allen SL, Koduru P, Brody JP, Hawson G, Rodwell R, Doody ML, Carnicero F, Reiter A, Goldman JM, Melo JV, Cross NC. The t(8;22) in chronic myeloid leukemia fuses BCR to FGFR1: transforming activity and specific inhibition of FGFR1 fusion proteins. *Blood* 2001;**98**:3778–83.